ADVANCED FUNCTIONAL MATERIALS
www.afm-journal.de

Designing Conductive Pyrrolidinium-Based Dual Network Gel Electrolytes: Tailoring Performance with Dynamic and Covalent Crosslinking

*Zviadi Katcharava, Torje E. Orlamünde, Lawrence T. Tema, Haobo Hong, Mario Beiner, Boyan Iliev, Anja Marinow, and Wolfgang H. Binder**

Transitioning toward a carbon-negative direction necessitates continued development and enhancement of existing lithium battery technologies. A key impediment for these technologies is the utilization of flammable organic solvent-based electrolytes, which pose significant safety risks. Furthermore, the recyclability of batteries has not reached the level required for transitioning to a circular economy. Here, poly(ionic liquid)-based dual network gel electrolytes are reported as safer and sustainable alternative materials. The materials employ both, dynamic (up to 45 mol%) and covalent crosslinking (up to 10 mol%), allowing the fabrication of mechanically stable gels with a high content (up to 65 wt%) of ionic liquid/salt both via thermal and photo polymerization. The dual nature of this network in interplay with other key components is systematically investigated. Mechanical stability (up to 0.7 MPa), combined with enhanced ionic conductivity (surpassing 10^{-4} S cm^{-1} at room temperature) is achieved via the synergetic combination of dynamic non-covalent and covalent crosslinking, resulting in improved electrochemical (up to 5 V) and thermal stability (reaching 300 °C) by the embedded ionic liquid. Moreover the presence of the dynamic crosslinks facilitates reprocessing at 70 °C without comrpomising the electrochemical performance, thus reaching full recyclability and reusability.

1. Introduction

Transporting ions through space in condensed soft matter is surely among the most important physical processes, generating materials with unparalleled properties.[1] Whereas ion-transporting materials based on small molecules, such as cyclic carbonates, are well known and used throughout society as charge-storage devices (batteries, supercapacitors), they present significant hurdles in view of mechanical endurance, flammability, and chemical stability during repeated cycling.[2] The quest for novel charge-transporting materials has therefore initiated intensified activities to combine a more stable ion-transporting property with enhanced mechanical properties, such as ionic liquids (ILs), polymeric ionic liquids (PILs), ion-gels and crosslinked gel-electrolytes.[3] In these materials, ionic moieties (e. g. imidazolium-, pyrrolidinium-moieties) are embedded into a surrounding polymer matrix, either linked covalently or noncovalently, leading to materials with ionic conductivities in the range of 1.6×10^{-4}–9.3×10^{-3} S cm^{-1} and E-moduli ranging from 30 kPa to 3.7 MPa.[4] Ion-gels represent a structural derivative from conventional gel materials, composed from nonconductive polymers or PILs, swollen by embedded ionic liquids, showcasing highly tunable properties driven by the specific combination of ionic liquid constituents and the gel matrix.[4b,5]

Z. Katcharava, T. E. Orlamünde, L. T. Tema, H. Hong, A. Marinow, W. H. Binder
Macromolecular Chemistry
Division of Technical and Macromolecular Chemistry
Faculty of Natural Sciences II (Chemistry Physics Mathematics)
Institute of Chemistry
Martin Luther University Halle-Wittenberg
von-Danckelmann-Platz 4, D-06120 Halle, Germany
E-mail: wolfgang.binder@chemie.uni-halle.de

M. Beiner
Fraunhofer Institute for Microstructure of Materials and Systems IMWS
Walter Hülse Str. 1, D-06120 Halle, Germany

B. Iliev
IoLiTec – Ionic Liquids Technologies GmbH
Im Zukunftspark 9, 74076 Heilbronn, Germany

The ORCID identification number(s) for the author(s) of this article can be found under https://doi.org/10.1002/adfm.202403487

DOI: 10.1002/adfm.202403487

In both, ion-gels and crosslinked gels, the conductivity[6] is strongly linked to the mechanical properties by the VTF-relation,[4b] deviating from low molecular weight ionic liquids, as an increased coupling of charge-transport to segmental movement of the polymers occurs.[7] Although coupling between polymer dynamics and counterion mobility leads to a favorable ion transport in PIL- soft materials above their glass transition, Tg, polymeric materials characterized by increased mechanical strength, often are displaying low or insufficient ion conductivities. Previously reported, solely covalently crosslinked systems thus show a drastic (orders of magnitude) reduction of conductivity,especially in highly covalently crosslinked system when compared to their less densely crosslinked counterparts.[8]

Thus the design of dual polymer networks by combination of covalent and/or dynamic crosslinks offers expanded opportunities for balancing conductivity and mechanical integrity in gel electrolytes, while simultaneously introducing advanced features like self-healing and/or reprocessability.[9] Incorporating non-covalent bonds, such as hydrogen bonding systems into gel-electrolytes can thus result in attractive dynamic properties, potentially decoupling mechanical properties from charge-transport, as then bonding dynamics is superimposed on the usually slower chain dynamics of the surrounding polymer-segments. However, a correlation of the density of dynamic bonds in relation to changes in both, ionic conductivity and mechanical properties has not been investigated systematically, still placing electrolyte design to a more trial-and-error-approach. We therefore consider the design of dual networks as important to achieve gel electrolytes with high ionic conductivity and good reprocessability, while simultaneously enhancing mechanical integrity, as exemplified in this work.

Major factors allowing to tune ion conductivity of gel materials include the choice of IL components[4a,10] along with the salt content.[7a,11] Pyrrolidinium-based ILs, despite some drawbacks in conductivity due to their higher viscosity, demonstrate notably enhanced electrochemical stability compared to their imidazolium analogs, while maintaining comparably high thermal stability.[12] Introducing fluorine containing functionalities (e.g. in cations/anions, polymer backbone, or crosslinkers) has been demonstrated to promote charge transport, enhance thermal and electrochemical stability, and positively affect the stability of the electrode/electrolyte interface.[11b,13] Embedding ionic liquids into crosslinked (either covalently- or non-covalently) gel electrolytes or block-copolymers results in materials where strongly different properties can be combined by copolymerization of monomers. Ionic liquid moieties, required as ion solvating and transporting units are thus combined with crosslinking points (tuning stiffness),[14] transient crosslinking points (such as supramolecular entities mediating self-healing),[4d,9c,15] dynamic covalent bonds (enabling reprocessing of vitrimers)[8b,16] or particles (modulating ion-transport).[17] A variety of crosslinked gel formulations have been proposed to enhance ionic conductivity while preserving robust mechanical properties in gel-electrolyte films. Recognizing the stabilizing effect of pyrrolidinium based IL on the solid interface layer (SEI),[18] Bieker et al. investigated the impact of the IL and salt content on the performance of tertiary crosslinked gel electrolytes (PEODA, Pyr_{14}TFSI, LiTFSI), reaching ion conductivities exceeding 1×10^{-3} S cm^{-1} (at 60 °C).[19] Crosslinking of imidazolium based monomers with PEGMA[20] or dispersing imidazolium ILs into 3D crosslinked ether-acrylate polymer matrix[21] led to the formation of crosslinked gel electrolytes with conductivities in the range of $2 - 7 \times 10^{-4}$ S cm^{-1} (at 25 °C) and Young modulus of 0.3 MPa. Xu and coworkers introduced a dynamic networks structure via a straightforward photopolymerization of a quadruple-hydrogen bonded (ureidopyrimidone, UPy)-containing monomers in junction with acrylate ether and imidazolium-based monomers. The resulting optimized gel electrolyte displayed an elevated ion conductivity of 3.8×10^{-3} S cm^{-1} (at 25 °C), while upholding a Youngs modulus of 1.5 MPa.[15c]

We here report on the systematic design of covalently crosslinked (*CL*) gel-electrolytes containing hydrogen bonds as additional, dynamic crosslinks (*DL*), to correlate directly to conductivity and strength. Focus is placed on pyrrolidinium-ILs, where three different sets of crosslinkers (hydrophobic; hydrophilic and fluorophobic) are investigated, in addition to the presence of a precise fraction of a dynamic crosslinker (a quadruple hydrogen bonding UPy moiety), recently found to be stable in ionic–liquid electrolytes,[22] thus transferring dynamic properties into the gel-electrolytes then impeding self-healing and strongly temperature-dependent properties. We consequently varied the nature and fraction of the covalent/dynamic crosslinker, in addition to the type and amount of the LiX-salt, further taking into account the method of crosslinking (thermal vs photochemical) to optimize the gel's performance, both in view of conductivity and mechanical properties. The finally discovered gel-electrolyte is electrochemically stable above 5 V, easy to prepare and to embed into electrodes, and exhibits a conductivity up to 4×10^{-4} S cm^{-1} (at 20 °C).

2. Results and Discussion

2.1. Gel Electrolyte Components and Preparation

In our quest to reach tunable properties of gels, intricately linked to the nature and amounts of the incorporated components, we have focused on a set of different components to optimize both, conductivity and mechanical strength, taking into account the individual properties of the liquid components, the mechanical strength and flexibility of the crosslinkers, as well as the amounts of covalent/dynamic crosslinks. The general procedure for preparing gel electrolytes and the embedded components is schematically presented in **Figure 1**a. Typically, a multicomponent gel precursor is dissolved in dry dichloromethane (DCM) and the mixture is spread onto a glass surface after removing the solvent. The so homogeneously distributed precursor is then polymerized via either thermal or photoinitiated polymerization techniques. This results in the formation of a homogenous polymer film, which combines dynamic interactions with covalent crosslinking and contains embedded ionic liquids. The selection of gel components is diverse (Figure 1b), with a particular emphasis on pyrrolidinium based IL-compounds, owing to their exceptional electrochemical stability window and superior thermal properties.[12,23]

We identified and considered the following key components to optimize the gel electrolytes:

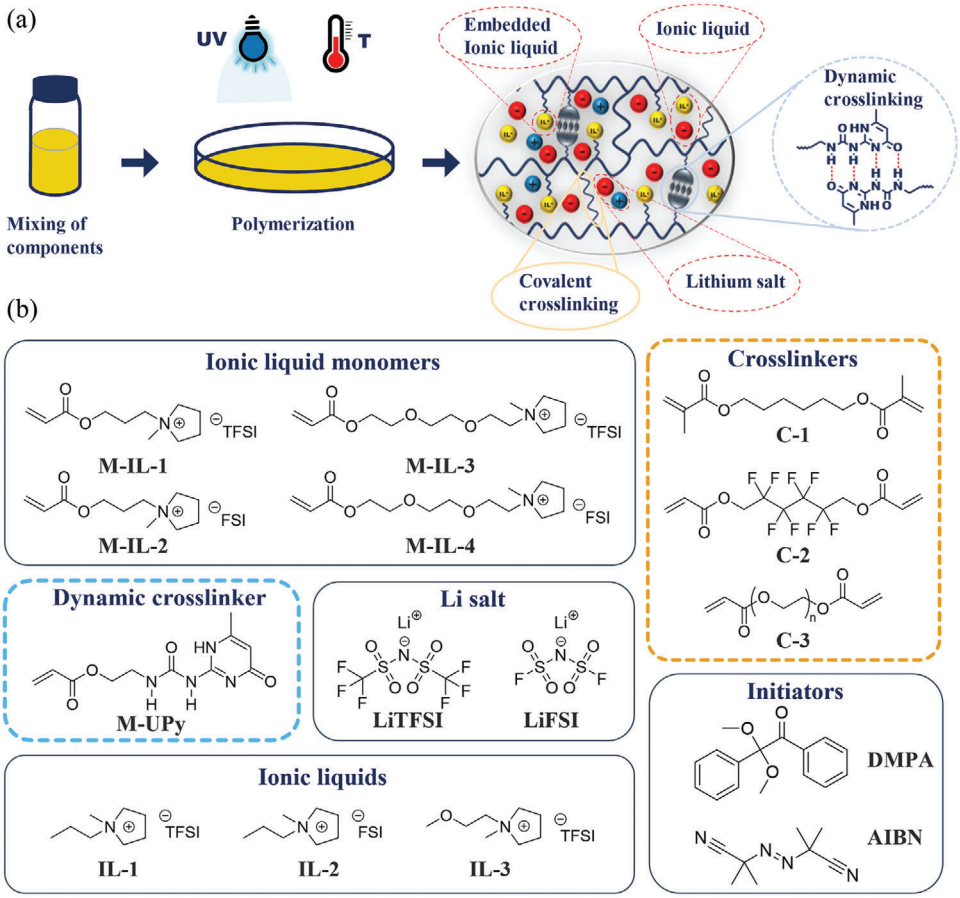

Figure 1. a) Schematical representation of gel electrolyte preparation and highlighted characteristic features, b) chemical structures of gel components.

i. *Covalent crosslinkers (CL):* 1,6-hexanediol dimethacrylate (**C-1**), 2,2,3,3,4,4,5,5-octafluoro-1,6-hexanediol diacrylate (**C-2**) and poly(ethylene glycol) diacrylate with a molecular weight of 700 Da (**C-3**) were selected as covalent crosslinkers for assessing the influence of fluorinated or ethylene oxide (EO) containing chains on the electrolytes' properties. To investigate the influence of the type of polymerization both thermal (AIBN) and photochemical (DMPA) initiators have been used.

ii. *Dynamic crosslinking (DL):* an acrylate-based monomer containing a quadruple hydrogen bonding UPy moiety, known for its ability to form stable 3D dynamic networks even in ionic environment (**M-UPy**, detailed synthesis in the Supporting Information) is used as a dynamic crosslinker. The rationale for integrating UPy moieties was to explore the possibility of introducing self-healing properties. It has been widely documented in the literature that the inclusion of quadruple hydrogen bonding is notably effective in realizing this property.[3d,24] Furthermore, we recently have proven the stability of the quadruple-hydrogen bonds in ionic liquid environment.[22] The presence of quadruple H-bonds facilitates the formation of a stable supramolecular 3D network, which enables comparison and investigation of the combined dynamic and covalent crosslinking, which isthe primary focus of this work.

iii. *IL monomers:* Pyrrolidinium-based compounds, attached to polymerizable acrylate groups and cation connected with different linker/spacer and containing either FSI or TFSI counterion were employed for the preparation of crosslinked gel electrolytes (compounds **M-IL-1**, **M-IL-2**, **M-IL-3** and **M-IL-4**, detailed synthetic procedures in ESI).

iv. *Ionic liquids:* pyrrolidinium-based ionic liquids (with varying counterion and structures, **IL-1**, **IL-2** and **IL-3**) were used, expecting a high thermal and electrochemical stability, when compared to the conventionally used imidazolium-ILs.

v. *Lithium salts:* LiTFSI and LiFSI were selected as additional salts for crosslinked gels, as they represent promising types of Li salt with high electrochemical stability.

The presence of numerous components in the gel electrolyte necessitates optimization to achieve the best performance without compromising key characteristics, such as mechanical properties or ionic conductivity. We focused on investigating the influence of the polymer precursor and the mobile phase on parameters such as the mechanical properties, the conductivity and the reprocessability of the resulting crosslinked gel electrolyte films. The polymer precursor is composed of the IL monomer, the UPy monomer and a covalent crosslinker, while the dual-component mobile phase consists of IL and Li salt (**Figure 2a**). After polymerization, the mixture results in transparent, self-

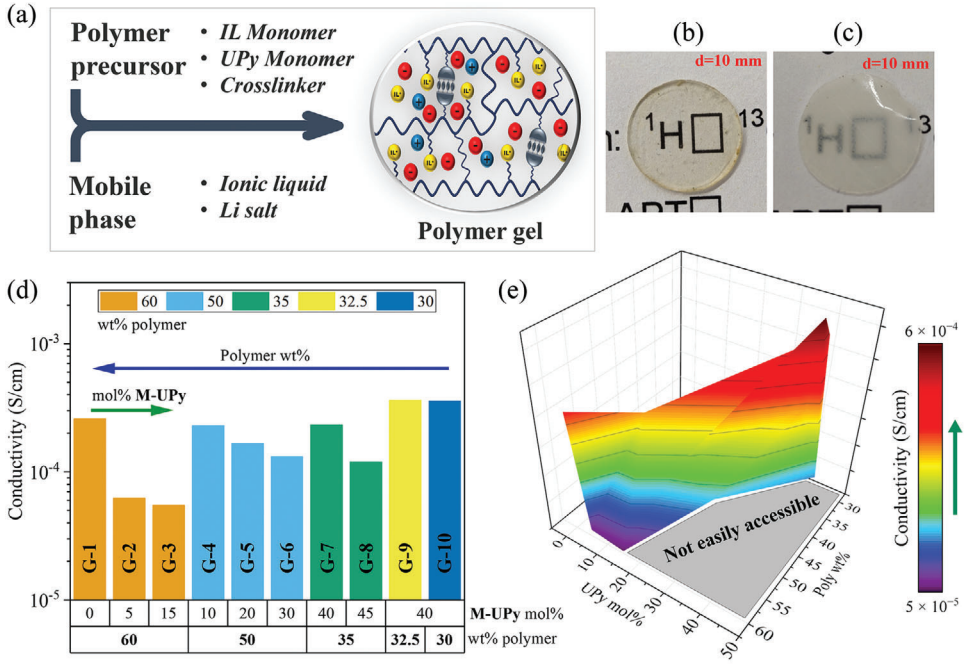

Figure 2. a) Schematic presentation of gel components divided into polymer precursor and mobile phase, b) gel electrolyte film with full conversion and incorporation of components, c) gel sample with incomplete incorporation of components, d) conductivity versus polymer content and UPy mol% (with respect to IL monomer) at RT and e) 3D map of compositions and corresponding relative conductivity.

standing films (Figure 2b). We were able to identify eventually incomplete polymerization/crosslinking by the formation of opaque films (Figure 2c) and thus exclude those samples from further testing.

2.2. Designing Gel Electrolytes: Tuning DL/CL Ratio for Improved Properties

To optimize conductivity, while preserving the mechanical integrity of the gel electrolyte films different components are systematically varied including the content of dynamic crosslinker (*DL*, using the UPy monomer in the range of 0–45 mol%), the type and the degree (0–10 mol%) of covalent crosslinker (*CL*), the content of polymer precursor (35–60 wt%) versus mobile phase (40–65 wt%), type of IL monomer, type/amount of the IL and added salt. The summary of gel compositions, along with corresponding components and ratios, is given in **Table 1**.

Increasing the ratio of *DL*/*CL* at a constant amount of *CL* (5 mol%) in the crosslinked gels reduces conductivity. This trend is depicted in Figure 2d, where the reduction of conductivity follows the order **G-1** > **G-2** > **G-3** with increasing UPy content from 0 to 15 mol% (with respect to combined monomers amount), while maintaining a constant weight ratio of the polymer/mobile phase (polymer wt% = 60) and keeping the *CL* molar content constant (5 mol%). Such behavior was anticipated by the presence of UPy, forming strong dynamic crosslinks to restrict chain dynamics and consequently reduce the mobility of ions.[15c,25] We further checked modifications in the ratio of polymer/IL-content: when the overall polymer content is reduced from 60 to 50 wt% (by increasing the weight ratio of the mobile phase), a similar trend is observed (**G-4** > **G-5** > **G-6**). However, the reduction of ionic conductivity is less pronounced because a significant contribution to the ion conductivity can be attributed to the mobile phase.

While increasing the content of the UPy monomer results in a decreased conductivity, the increased mechanical properties are the tradeoff, additionally allowing incorporation of more ionic liquid/Li salt mixture into the electrolyte. Thus **G-1**, containing no UPy moieties, exhibits extremely poor mechanical properties, with the corresponding film easily breaking upon handling unlike samples with the embedded dynamic interactions. We further observed a strong dependency of the possibility to introduce the dynamic crosslinker (UPy) into the initial polymer composition: when the overall polymer content is fixed at 60 wt%, the upper limit of the UPy-monomer as a *DL* is 15 mol%, as at higher contents the precursor mixture is not completely dissolved. Reducing the polymer content (increasing the amount of mobile phase) is positively affecting the solubility of the UPy monomer and allows its incorporation of up to 30 mol% into the gel electrolyte. In the optimized compositions the content of the dynamic crosslinker, UPy, therefore can reach up to 40 mol%, still maintaining the high RT conductivity (above 10^{-4} S cm^{-1}) and reaching good mechanical properties (**G-7** and **G-8**). With a further increase in the content of mobile phase (**IL**), the conductivity remains largely unchanged (**G-9** and **G-10**), while the mechanical properties deteriorate, making sample handling difficult. Thus, the optimal composition of the gel electrolyte for our system was achieved with a polymer network content of ≈35 wt% and a content of the dynamic crosslinker, UPy, of 40 mol% (with IL monomer 60 mol% and 95:5 monomer: *CL* ratio). The observed trends in conductivity can be more effectively visualized on a 3D map (Figure 2e). High conductivity values are reached when either the content of the mobile phase is high, or the UPy content is relatively low. The areas highlighted in grey indicate

Table 1. Gel electrolyte compositions, component ratios and mode of crosslinking (dynamic crosslinks (*DL*, M-UPy); covalent crosslinks (*CL*, C).

Sample	Monomer	Crosslinker	Molar ratio M-IL/M-UPy/C			Ionic liquid	IL [wt%]	Li salt	Li salt [wt%]
G-1	**M-IL-1**	**C-1**	95:	0	: 5	**IL-1**	30.00	LiTFSI	10.00
G-2	**M-IL-1**	**C-1**	90:	5	: 5	**IL-1**	30.00	LiTFSI	10.00
G-3	**M-IL-1**	**C-1**	81:	14	: 5	**IL-1**	30.00	LiTFSI	10.00
G-4	**M-IL-1**	**C-1**	86:	10	: 5	**IL-1**	37.50	LiTFSI	12.50
G-5	**M-IL-1**	**C-1**	76:	19	: 5	**IL-1**	37.50	LiTFSI	12.50
G-6	**M-IL-1**	**C-1**	67:	29	: 5	**IL-1**	37.50	LiTFSI	12.50
G-7	**M-IL-1**	**C-1**	52:	43	: 5	**IL-1**	48.70	LiTFSI	17.50
G-8	**M-IL-1**	**C-1**	57:	38	: 5	**IL-1**	48.70	LiTFSI	16.25
G-9	**M-IL-1**	**C-1**	57:	38	: 5	**IL-1**	50.63	LiTFSI	16.88
G-10	**M-IL-1**	**C-1**	57:	38	: 5	**IL-1**	52.50	LiTFSI	17.50
G-11	**M-IL-1**	**C-1**	90:	0	: 10	**IL-1**	36.50	LiTFSI	13.50
G-12	**M-IL-1**	**C-1**	54:	36	: 10	**IL-1**	45.00	LiTFSI	15.00
G-13	**M-IL-4**	**C-2**	58:	37	: 5	**IL-2**	48.70	LiFSI	16.25
G-14	**M-IL-4**	**C-1**	58:	37	: 5	**IL-2**	48.70	LiFSI	16.25
G-15	**M-IL-1**	**C-3**	57:	38	: 5	**IL-1**	48.70	LiTFSI	16.25
G-16	**M-IL-1**	**C-1**	57:	38	: 5	**IL-1**	44.85	LiTFSI	20.15
G-17	**M-IL-1**	**C-1**	57:	38	: 5	**IL-1**	40.00	LiTFSI	25.00
G-18	**M-IL-1**	**C-1**	57:	38	: 5	**IL-3**	48.70	LiTFSI	16.25
G-19	**M-IL-3**	**C-1**	57:	38	: 5	**IL-1**	48.70	LiTFSI	16.25
G-20	**M-IL-3**	**C-1**	57:	38	: 5	**IL-1**	48.70	LiTFSI	16.25
G-21	**M-IL-1**	**C-1**	57:	38	: 5	**IL-1**	48.70	LiTFSI	16.25
G-22	**M-IL-1**	**C-1**	57:	38	: 5	**IL-1**	48.70	LiTFSI	16.25
G-23	**M-IL-2**	**C-1**	57:	38	: 5	**IL-2**	47.50	LiFSI	13.72
G-24	**M-IL-2**	–	60:	40	: 0	**IL-2**	47.50	LiFSI	13.72

regions that cannot be easily accessed due to poor solubility of the components or the formation of mechanically weak gels.

The influence of dynamic crosslinks (*DL*) on the mechanical stability of the crosslinked gel electrolytes is clearly demonstrated by tensile testing. **Figure 3a** illustrates the stress to strain curves of **G-11** (M-IL:M-UPy:C = 90:00:10), **G-8** (M-IL:M-UPy:C = 57:38:05) and **G-12** (M-IL:M-UPy:C = 54:36:10). A solely covalently crosslinked gel devoid of dynamic crosslinkers (**G-11**) exhibits extremely weak toughness (>1 J cm^{-3}) and tensile strength, fracturing at low 10% strain. Introduction of hydrogen bonding through **M-UPy**, enabling additional dynamic crosslinking, dramatically improves elasticity and toughness (40–50 J cm^{-3}), with **G-8** achieving an elongation up to 270%. Moreover, covalent crosslinking (*CL*) further enhances tensile strength. While increasing the crosslinking density (changing the monomers: *CL* molar ratio from 95:5 to 90:10) increases strength significantly, it comes at the cost of reduced elasticity, resulting in fracture at 115% strain (**G-12**).

2.3. Tailoring Ionic Conductivity in Crosslinked Gel Electrolyte: Effects of Li Salt, Ionic Liquid and Type of Covalent Crosslinker

One of the crucial factors governing the electrolyte's performance is the concentration of the lithium salt.[11a,19,26] While low concentrations of Li salt reduce the initial solubility of the UPy monomer, we focused on high salt contents to explore the optimal range for a functionable electrolyte. Figure 3b depicts RT conductivities of three crosslinked gel electrolytes (**G-8**, **G-16**, and **G-17**) containing increasing LiTFSI content (16.25, 20.15, and 25.00 wt%, respectively). Exceeding 20 wt% LiTFSI leads to a significant drop in conductivity, from 1.06×10^{-4} S/cm (**G-8**) to 3.6×10^{-5} S cm^{-1} (**G-17**). Additionally, the type of the IL-moiety integrated as a monomer or within the mobile phase can significantly influence gel performance. Ethylene oxide is widely acknowledged for its beneficial impact on ionic transportation, facilitating lithium-ion movement.[27] Various materials based on PEO/EO structures have shown promise as electrolytes.[17d,28] Thus, within the scope of this study we introduced different EO moieties to systematically investigate their influence on the charge transfer properties of the resulting gel electrolytes. Two samples, **G-8** and **G-18** were prepared containing 1-methyl-1-propylpyrrolidinium bis(trifluoromehylsulfonyl)imide (**IL-1**) and 1-(2-methoxyethyl)−1-methylpropylpyrrolidinium bis(trifluoromethylsulfonyl)imide (**IL-3**), respectively. The incorporation of **IL-3** with a methoxyethyl group resulted in minor changes of conductivity (Figure 3c) while RT values are maintained above 10^{-4} S cm^{-1}.

Furthermore, the impact of the covalent crosslinker type on gel conductivity was also investigated. Notably, poly(ethylene glycol) diacrylate (Mn = 700 Da) (**C-3**) was probed as a *CL*, displaying higher Li-ion transport capabilities compared to 1,6-hexanediol

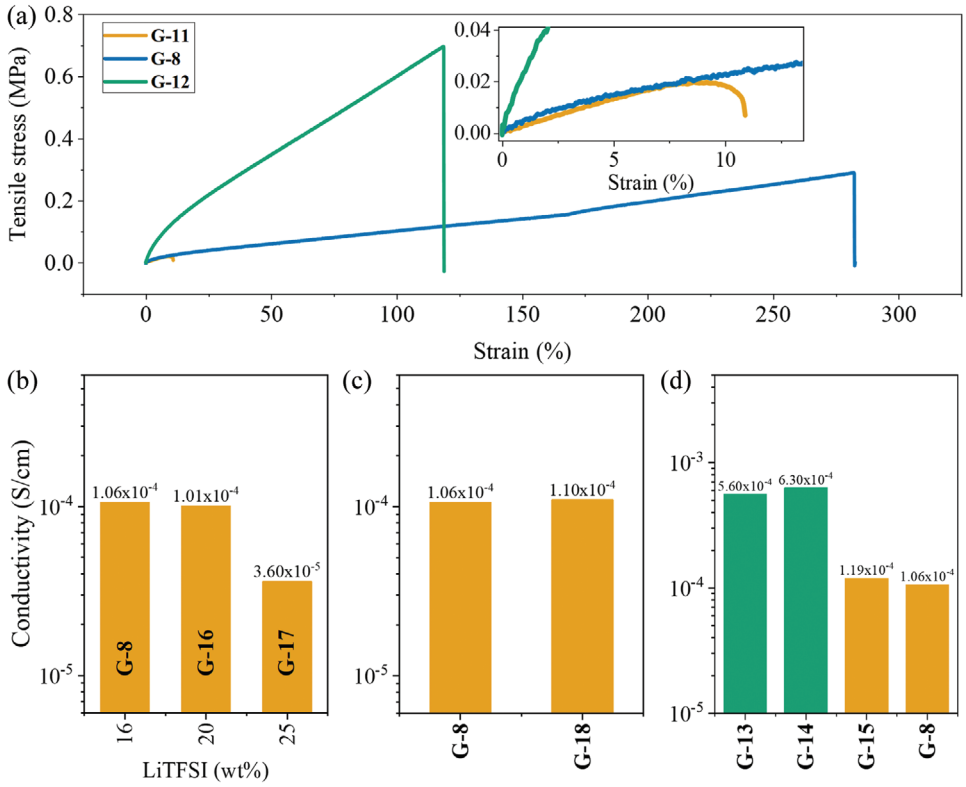

Figure 3. a) Tensile test of **G-11**, **G-8** and **G-12**, conductivity at RT of b) **G-8**, **G-16** and **G-17**, c) **G-8** and **G-18** and d) **G-13**, **G-14**, **G-15**, and **G-8**.

dimethacrylate (**C-1**) due to higher molecular weight and the presence of ethylene oxide repeating units.[29] Figure 3d depicts a negligible changes in conductivity (**G-15** vs **G-8**) due to the low concentration of covalent crosslinker (5:95 molar ratio to total monomers). Moreover, using the fluorinated *CL* (**C-2**), known for its improved electrochemical stability,[30] was tested in crosslinked gels based on **M-IL-4** (characterized by an EO-based linker between the cation and the acrylate group). Room temperature conductivity measurements of **G-13** (crosslinker **C-2**) and **G-14** (crosslinker **C-1**) in Figure 3d revealed only minor changes between the fluorinated and non-fluorinated crosslinker (σ(**G-13**) = 5.60×10^{-4} S cm^{-1}, σ(**G-14**) = 6.3×10^{-4} S cm^{-1}). These findings highlight that within the investigated range, the specific nature of the covalent crosslinker choice is not significantly affecting the conductivity of the resulting gel-electrolytes.

2.4. Impact of Linker Type (EO vs Aliphatic) in Ionic Liquid Monomers and Polymerization Method on Ionic Conductivity

We further examined the impact of EO-based linkers between the cation and the acrylate group (**M-IL-1** and **M-IL-3**), as this is postulated to display potential to improve ion conductivities.[3i,31] Broadband dielectric spectroscopy (BDS) measurements from −20 to 70 °C were conducted on crosslinked gels based on **M-IL-1** (**G-22**) and **M-IL-3** (**G-19**) to understand their behavior across a wide temperature range. As expected, the typical frequency versus conductivity curves in **Figure** 4a reveal a gradual decrease in conductivity with decreasing temperature for **G-19** (based on **M-IL-3**). The positive influence of EO groups is evident in Figure 4b, where the values for **G-19** considerably exceed **G-22**, reaching 1×10^{-3} S cm^{-1} at 70 °C for both compositions. Additionally, we examined the impact of the polymerization method on the performance of the crosslinked gels. Similar compositions prepared via both thermal and photo polymerization methods indicate (Figure 4c,d) that the conductivity remains largely unaffected. Notably, photo-polymerization offers distinct advantages due to its drastically reduced polymerization time, enabling high throughput sample preparation. Furthermore, direct in situ polymerization leads to enhanced electrolyte, electrode contact, enabling facilitated charge transport.[32] The temperature dependence of conductivity can be described via the Vogel−Tammann−Fulcher (VTF) model.[6c,e,29a] The obtained behavior of crosslinked gels fit well within the model with very high adjusted r square values (detailed fitting parameters available in Supporting information).

To ensure complete polymerization and network formation, FTIR spectroscopy was employed (Figure 4e). Analyzing the spectrum of selected gels and the starting monomer **M-IL-1** reveals a characteristic peak which corresponds to the C=C stretching vibration of the acrylate double bond (1610–1640 cm^{-1} region),[30,33] highlighted in yellow. The disappearance of this peak is clearly evident in the zoomed-in section after polymerization, confirming the full conversion of monomers to polymer network. Additionally, gels were analyzed via a reflection electron microscope (REM), further providing insights into the materials morphology. Figure 4f reveals a homogenous and smooth surface structure (around the sample holder region). Although there are

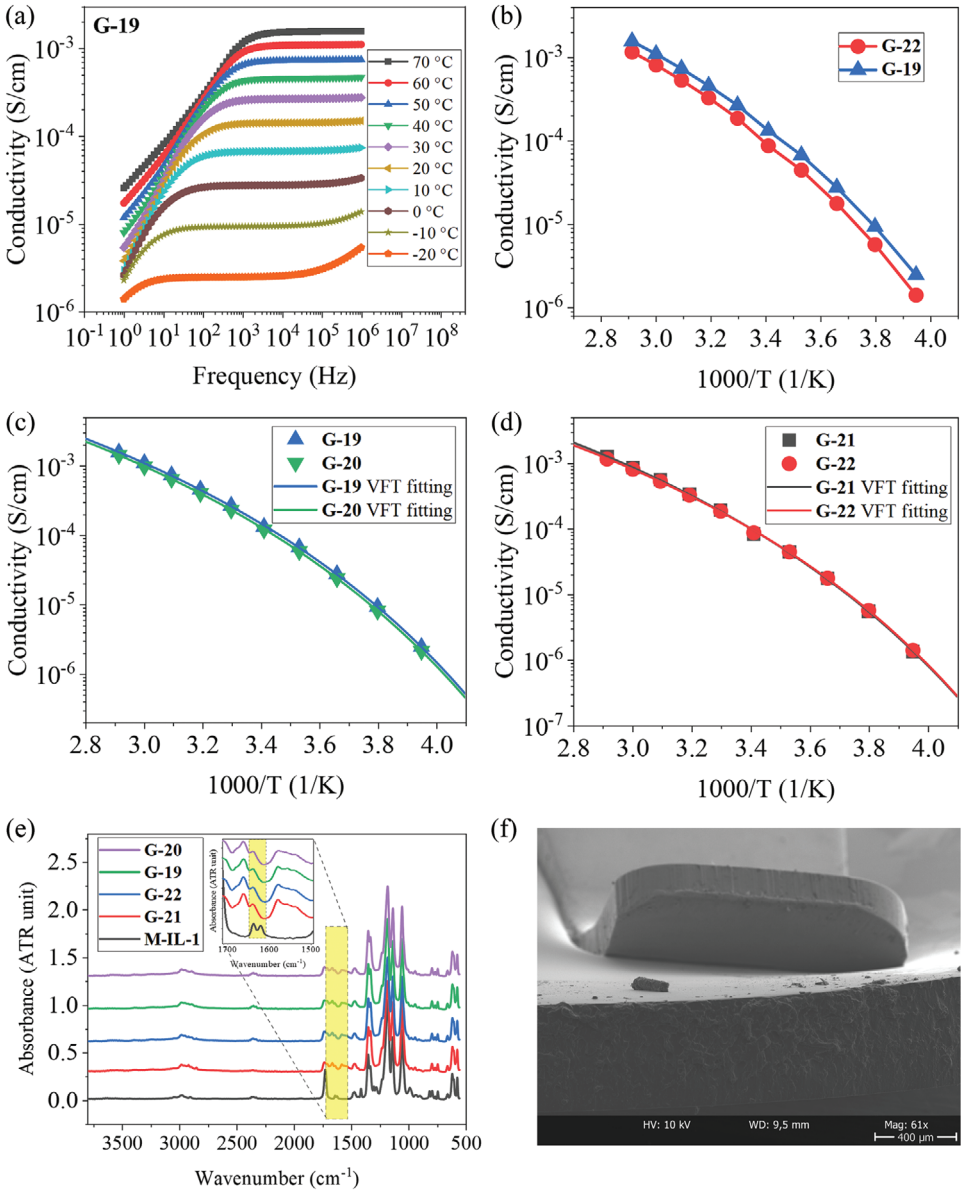

Figure 4. a) BDS measurement of **G-19** in the temperature range of –20–70 °C with 10 °C increments, the frequency range between 1 to 10^6 Hz, Conductivity as a function of temperature and VTF fitting of b) **G-19**, **G-20** and c) **G-21**, **G-22**, d) comparison of **G-19** and **G-22**, e) FT-IR spectrum of **G-19**, **G-20**, **G-21**, **G-22**, and **M-IL-1**, e) reflection electron microscope (REM) image of **G-21**.

minor inhomogeneities observed in the cross-section, these are likely attributed to the sample cutting after polymerization.

Both, the presence of ethylene oxide groups and the counterion type significantly impact the ionic conductivity of dually crosslinked gel electrolytes. **Figure 5a** (displaying conductivity at 20 °C) clearly shows this correlation: gels with the FSI counterion exhibit higher conductivity compared to those with TFSI (**G-22** vs **G-23** and **G-19** vs **G-14**), which is in accordance with the literature.[10,11b,34] Additionally, introducing EO-based linker leads to further enhancement of performance (**G-23** vs **G-14** and **G-19** vs **G-22**). Interestingly, completely removing the covalent crosslinking can almost double the conductivity (**G-22** vs **G-24**) and additionally enable self-healing/reprocessing ability. While this approach allows advanced functionalities, it sacrifices mechanical performance and results in reduced structural integrity. Therefore, finding a balance between electrochemical and physical properties is crucial.

2.5. Stability of the Optimized Dual Network Gel Electrolytes: Flammability, Thermal/ Electrochemical Stability and Reprocessability

Beyond conductivity, practical applications of crosslinked gel electrolyte demand thermal stability, non-flammability, and a wide electrochemical window.[35] Figure 5b displays TGA

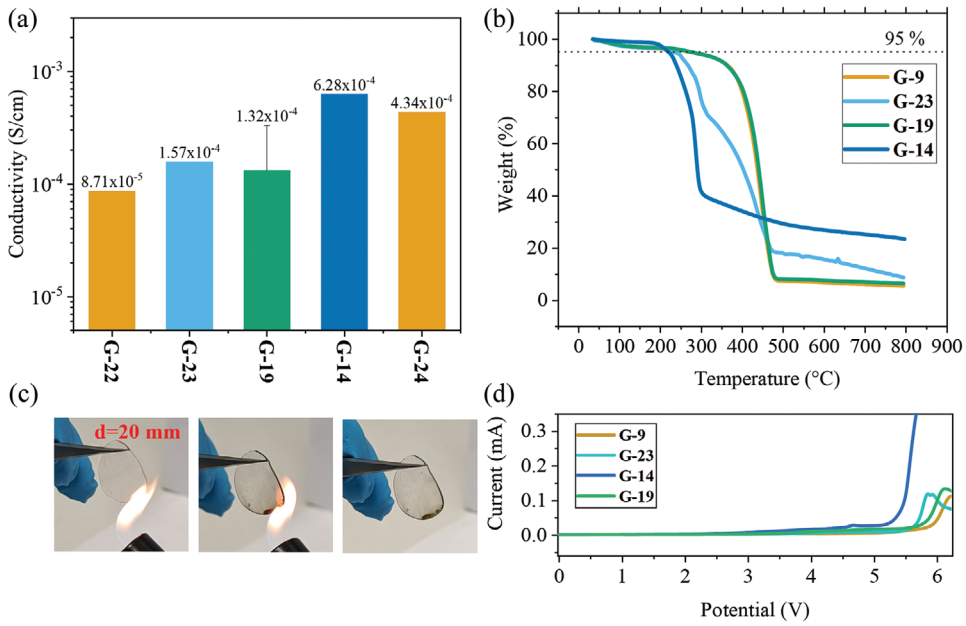

Figure 5. a) Ionic conductivity of **G-22**, **G-23**, **G-19**, **G-14**, and **G-24** at 20 °C, b) TGA measurements of **G-9**, **G-23**, **G-19**, and **G-14**, c) flammability test of gel electrolyte and d) LSV measurements of **G-9**, **G-23**, **G-14**, and **G-19**.

measurements of all four types of monomer-based gels **G-9**, **G-23**, **G-19**, and **G-14**. Samples with TFSI counterion (**G-9** and **G-19**), irrespective of the chosen linker group in the monomer, demonstrate superior thermal stability up to 300 °C. While FSI-based counterparts (**G-23** and **G-14**) exhibit a lower limit ≈200 °C, this still exceeds typical operating temperatures in most applications. Figure 5c illustrates the experiment for testing the flammability. ILs and polymers are recognized as safer alternatives due to their non-flammability features.[36] Upon direct flame exposure, the crosslinked gel specimens resist ignition, and no flames are observable once the source is removed. This inherent safety feature is very critical for battery applications, where flammability risks are associated with dangerous processes.[37] Another key parameter is the electrochemical stability window. All samples were investigated by linear sweep voltammetry and the results shown in Figure 5d display excellent stability above 5 V that allows the potential application in next-generation high voltage batteries.

The absence of covalent crosslinking in **G-24** unlocks several key improvements, presumably due to increased polymer chain mobility. **Figure** 6a demonstrates remarkably higher conductivity of **G-24** compared to its covalently crosslinked counterpart (**G-23**), with almost an order of magnitude increase across the entire temperature range. Furthermore, another advanced functionality of **G-24** is its ability to be reprocessed, addressing the growing concern of material sustainability.[38] Reprocessing is achieved simply by applying heat and pressure to the cut polymer gel prices (Figure 6b), and after 4 h at 70 °C the integrity and functionalities of the specimen are restored. This is evident in Figure 6a, where the conductivity measurement before and after reprocessing are overlapping. This successful and efficient reprocessing capability significantly reduces material waste and promotes a more sustainable approach.

3. Conclusion

In summary, a series of pyrrolidinium based poly(ionic liquid) gel electrolytes containing either covalent (*CL*, up to 10 mol%) and/or dynamic (UPy-H-bonds, *DL*, up to 45 mol%) crosslinks have been successfully synthesized. The presence of the dynamic

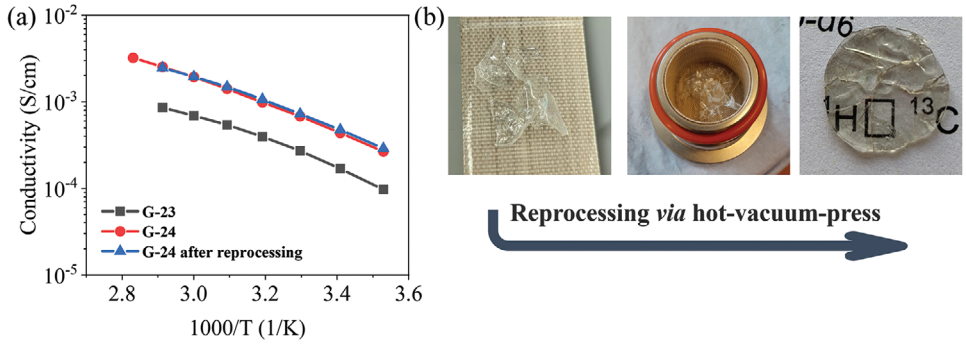

Figure 6. a) Ionic conductivity of **G-23**, **G-24**, and **G-24** after reprocessing, b) reprocessing of **G-24** via hot-vacuum-press at 70 °C for 4 h.

network enables higher contents of the added ionic liquid (IL) mobile phase as required to reach good conductivites (up to 65 wt% – IL/Li salt) within the gel without deteriorating mechanical properties. The tensile strength is fully adjustable ranging from 0.02 MPa (no UPy, 10 mol% covalent crosslinking); 0.29 MPa (with UPy, 5 mol% covalent crosslinking); 0.70 MPa (with UPy, 10 mol% covalent crosslinking). Synergetic effects of *CL*/*DL* crosslinking led to advanced functionalities including reprocessability, self-healing ability while simultaneously maintaining high ionic conductivity (exceeding 10^{-4} S cm^{-1} at RT). The influence of the ratio of dynamic/covalent crosslinks along with variation of relevant components has been systematically optimized. The so generated gels exhibit exceptional thermal stability, reaching up to 300 °C for TFSI containing compositions, surpassing their FSI-based counterparts that remain stable above 200 °C. Moreover, they demonstrate superior electrochemical stability, withstanding above 5 V, and are non-flammable. PIL gels offer versatility and can be prepared via both thermal and photopolymerization techniques, while maintaining excellent conductivity in the mS range at elevated temperatures. As we navigate through the intricacies of ion–gels, we can unravel the potential these materials hold for shaping the landscape of modern materials science and engineering. Based on such systematic approaches it can be hoped that with these combined properties, poly(ionic liquid) gels emerge as promising candidates for next-generation battery applications.

4. Experimental Section

Poly(ionic liquid) gels were synthesized with the following procedure: dry components were mixed in dry DCM and stirred in a closed vial until a clear solution was formed. Solvent was removed under reduced pressure. The mixture was transfered into glovebox, spread on the glass surface and polymerized at 75 °C for 16 h (AIBN, thermal initiation) or under UV light (365 nm, 4-watts, distance from the lamp 10–20 mm) for 1 h (DMPA, photopolymerization). Formed gels were removed from the glass and cut into round shapes with various diameters.

Thermogravimetric analysis (TGA): TGA was conducted on Netzsch TG 209 F3. Samples (5–15 mg) were placed in alumina crucibles and heated from 35 °C to 800 °C with the heating rate of 10 K min^{-1} under nitrogen atmosphere (flow rate 20 mL min^{-1}). The NETZSCH Proteus was used for analyzing the recorded data.

Fourier-Transform Infrared Spectroscopy (FT-IR): FT-IR analysis was conducted using attenuated total reflection technique on VERTEX 70 v FT-IR Spectrometer (Bruker) equipped with the golden gate diamond ATR unit. Measurements were conducted at room temperature and covered spectral range was from 550 to 4000 cm^{-1}.

Broadband Dielectric Spectroscopy (BDS): Novocontrol "Alpha analyzer" was used for investigating ionic conductivities. PIL gels were placed between two brass electrodes (d = 20 mm) and the thickness of each sample gel was measured individually. Measuring cell was placed in a cryostat with a constant flow of dry nitrogen. Ionic conductivity was recorded in the frequency range 1–10^6 Hz and different temperatures. Ion conductivity values were extracted from the plateau of σ versus T.

Linear Sweep Voltammetry (LSV): LSV measurements were conducted in a glovebox using potentiostat Autolab PGSTAT 204 with FRA32M module running on Nova 2.1.5 Software. A sample (10 mm diameter) was placed between stainless steel electrodes and measurement was conducted in the range of 0 – 8 V at 1 mV s^{-1} rate. Before each measurement, both electrodes are polished with 1 and 0.3 µm aluminum oxide suspension for 5 min.

Tensile: Tensile tests were performed using a universal testing machine Instron at room temperature in a normal laboratory condition with the strain rate of 20 mm min^{-1}.

Supporting Information

Supporting Information is available from the Wiley Online Library or from the author.

Acknowledgements

The authors are grateful to NorcSi GmbH for conducting REM measurements and Prof. Dr. Michael Bron for allowing LSV measurements. Authors acknowledge IoLiTec GmbH and Dr. Thomas Schubert for providing ILs and lithium salts. W.H.B. thanks the DFG project INST 271/444-1 FUGG for financial support; the DFG-Project BI1337/16-1; BI 1337/14-1 and the GRK 2670, W69000789, ProjectNr 436494874. WHB and ZK thank the European Transition Funds (JTC) for financial support. This research was developed under the framework of the BAT4EVER project. This project has received funding from the European Union's Horizon 2020 research and innovation programme under grant agreement No 957 225.

Open access funding enabled and organized by Projekt DEAL.

Conflict of Interest

The authors declare no conflict of interest.

Data Availability Statement

The data that support the findings of this study are available in the supplementary material of this article.

Keywords

gel electrolytes, poly(ionic liquid)s, re-processing, self-healing

Received: February 27, 2024
Revised: May 15, 2024
Published online: June 12, 2024

[1] a) S. M. Chen, K. H. Wen, J. T. Fan, Y. S. Bando, D. Golberg, *J. Mater. Chem. A* **2018**, *6*, 11631; b) S. S. Liang, W. Q. Yan, X. Wu, Y. Zhang, Y. S. Zhu, H. W. Wang, Y. P. Wu, *Solid State Ion* **2018**, *318*, 2; c) H. Yang, N. Q. Wu, *Energy Sci. Eng.* **2022**, *10*, 1643.

[2] A. L. Yang, C. Yang, K. Xie, S. Xin, Z. Xiong, K. Y. Li, Y. G. Guo, Y. You, *ACS Energy Lett.* **2023**, *8*, 836.

[3] a) M. Forsyth, L. Porcarelli, X. Wang, N. Goujon, D. Mecerreyes, *Acc. Chem. Res.* **2019**, *52*, 686; b) K. Xu, *Chem. Rev.* **2014**, *114*, 11503; c) A. K. Tripathi, *Mater. Today Energy* **2021**, *20*, 100643; d) A. Marinow, Z. Katcharava, W. H. Binder, *Polymers* **2023**, *15*, 1145; e) H. Y. Liao, W. Z. Zhong, T. Li, J. L. Han, X. Sun, X. L. Tong, Y. Q. Zhang, *Electrochim. Acta* **2022**, *404*, 139730; f) X. Ma, J. Yu, Y. Hu, J. Texter, F. Yan, *Ind. Chem. Mater.* **2023**, *1*, 39; g) Y. L. Hu, X. X. Xie, W. Li, Q. Huang, H. Huang, S. M. Hao, L. Z. Fan, W. D. Zhou, *ACS Sustainable Chem. Eng.* **2023**, *11*, 1253; h) X. Fan, S. Liu, Z. Jia, J. J. Koh, J. C. C. Yeo, C. G. Wang, N. E. Surat'man, X. J. Loh, J. L. Bideau, C. He, Z. Li, T. P. Loh, *Chem. Soc. Rev.* **2023**, *52*, 2497; i) M. Palluzzi, A. Tsurumaki, H. Adenusi, M. A. Navarra, S. Passerini, *Energy Mater.* **2023**, *3*, 300049; j) K. Aruchamy, S. Ramasundaram, S. Divya, M. Chandran, K. Yun, T. H. Oh, *Gels* **2023**, *9*, 585.

[4] a) H. Porthault, G. Piana, J. M. Duffault, S. Franger, *Electrochim. Acta* **2020**, *354*, 136632; b) B. X. Tang, S. P. White, C. D. Frisbie, T. P. Lodge, *Macromolecules* **2015**, *48*, 4942; c) T. Huang, M. C. Long, X. L. Wang, G. Wu, Y. Z. Wang, *Chem. Eng. J.* **2019**, *375*, 122062; d) P. Guo, A. Su, Y. Wei, X. Liu, Y. Li, F. Guo, J. Li, Z. Hu, J. Sun, *ACS Appl. Mater. Interfaces* **2019**, *11*, 19413.

[5] a) T. P. Lodge, T. Ueki, *Acc. Chem. Res.* **2016**, *19*, 2107; b) J. Lee, L. G. Kaake, J. H. Cho, X. Y. Zhu, T. P. Lodge, C. D. Frisbie, *J. Phys. Chem. C* **2009**, *113*, 8972.
[6] a) S. Sharick, J. Koski, R. A. Riggleman, K. I. Winey, *Macromolecules* **2016**, *49*, 2245; b) J. H. Choi, Y. S. Ye, Y. A. Elabd, K. I. Winey, *Macromolecules* **2013**, *46*, 5290; c) B. A. Paren, N. Nguyen, V. Ballance, D. T. Hallinan, J. G. Kennemur, K. I. Winey, *Macromolecules* **2022**, *55*, 4692; d) Y. S. Ye, J. H. Choi, K. I. Winey, Y. A. Elabd, *Macromolecules* **2012**, *45*, 7027; e) T. L. Chen, P. M. Lathrop, R. Sun, Y. A. Elabd, *Macromolecules* **2021**, *54*, 8780.
[7] a) Z. Zhang, D. Lin, V. Ganesan, *J. Polym. Sci.* **2021**, *60*, 199; b) V. Ganesan, *Mol. Syst. Des. Eng.* **2019**, *4*, 280; c) C. Iacob, A. Matsumoto, M. Brennan, H. Liu, S. J. Paddison, O. Urakawa, T. Inoue, J. Sangoro, J. Runt, *ACS Macro Lett.* **2017**, *6*, 941; d) F. Frenzel, W. H. Binder, J. R. Sangoro, F. Kremer, in *Dielectric Properties of Ionic Liquids* (Eds: M. Paluch, F. Kremer), Springer International Publishing, Switzerland **2016**, Ch. Chapter 5, p. 115.
[8] a) R. L. Weber, M. K. Mahanthappa, *Soft Matter* **2017**, *13*, 7633; b) R. Kato, P. Mirmira, A. Sookezian, G. L. Grocke, S. N. Patel, S. J. Rowan, *ACS Macro Lett.* **2020**, *9*, 500.
[9] a) A. J. D'Angelo, M. J. Panzer, *Chem. Mater.* **2019**, *31*, 2913; b) Y. Zhang, M. Li, B. Qin, L. Chen, Y. Liu, X. Zhang, C. Wang, *Chem. Mater.* **2020**, *32*, 6310; c) C. Wang, R. J. Li, P. Chen, Y. S. Fu, X. Y. Ma, T. Shen, B. J. Zhou, K. Chen, J. J. Fu, X. F. Bao, W. W. Yan, Y. Yang, *J. Mater. Chem. A* **2021**, *9*, 4758; d) X. Tian, P. Yang, Y. Yi, P. Liu, T. Wang, C. Shu, L. Qu, W. Tang, Y. Zhang, M. Li, B. Yang, *J. Power Sources* **2020**, *450*, 227629.
[10] M. Brinkkötter, E. I. Lozinskaya, D. O. Ponkratov, P. S. Vlasov, M. P. Rosenwinkel, I. A. Malyshkina, Y. Vygodskii, A. S. Shaplov, M. Schönhoff, *Electrochim. Acta* **2017**, *237*, 237.
[11] a) N. Molinari, J. P. Mailoa, B. Kozinsky, *Chem. Mater.* **2018**, *30*, 6298; b) Q. Huang, Y.-Y. Lee, B. Gurkan, *Ind. Eng. Chem. Res.* **2019**, *58*, 22587; c) M. Martinez-Ibañez, N. Boaretto, A. Santiago, L. Meabe, X. Wang, O. Zugazua, I. Raposo, M. Forsyth, M. Armand, H. Zhang, *J. Power Sources* **2023**, *557*, 232554.
[12] a) H. Qi, Y. Ren, S. Guo, Y. Wang, S. Li, Y. Hu, F. Yan, *ACS Appl. Mater. Interfaces* **2020**, *12*, 591; b) L. M. McGrath, J. F. Rohan, *Molecules* **2020**, *25*, 6002.
[13] a) X. Fan, L. Chen, X. Ji, T. Deng, S. Hou, J. Chen, J. Zheng, F. Wang, J. Jiang, K. Xu, C. Wang, *Chem* **2018**, *4*, 174; b) Q. Liu, C.-W. Hsu, T. L. Dzwiniel, K. Z. Pupek, Z. Zhang, *Chem. Commun.* **2020**, *56*, 7317; c) N. Xu, J. Shi, G. Liu, X. Yang, J. Zheng, Z. Zhang, Y. Yang, *J. Power Sources Adv.* **2021**, *7*, 100043.
[14] F. Baskoro, H. Q. Wong, H. J. Yen, *ACS Appl. Energy Mater.* **2019**, *2*, 3937.
[15] a) R. Tamate, M. Watanabe, *Sci. Technol. Adv. Mater.* **2020**, *21*, 388; b) C. Li, R. Bhandary, A. Marinow, D. Ivanov, M. Du, R. Androsch, W. H. Binder, *Polymers* **2022**, *14*, 4090; c) F. Chen, C. Guo, H. Zhou, M. W. Shahzad, T. X. Liu, S. Oleksandr, J. Sun, S. Dai, B. B. Xu, *Small* **2022**, *18*, 2106352.
[16] a) Z. Katcharava, X. Zhou, R. Bhandary, R. Sattler, H. Huth, M. Beiner, A. Marinow, W. H. Binder, *RSC Adv.* **2023**, *13*, 14435; b) X. Cao, P. Zhang, N. Guo, Y. Tong, Q. Xu, D. Zhou, Z. Feng, *RSC Adv.* **2021**, *11*, 2985; c) F. Li, G. T. M. Nguyen, C. Vancaeyzeele, F. Vidal, C. Plesse, *ACS Appl. Polym. Mater.* **2023**, *5*, 529; d) L. Wan, X. Cao, X. Xue, Y. Tong, S. Ci, H. Huang, D. Zhou, *Energy Technol.* **2021**, *10*, 2100749.
[17] a) A. Marie, B. Said, A. Galarneau, T. Stettner, A. Balducci, M. Bayle, B. Humbert, J. L. Bideau, *Phys. Chem. Chem. Phys.* **2020**, *22*, 24051; b) Z. Katcharava, A. Marinow, R. Bhandary, W. H. Binder, *Nanomaterials* **2022**, *12*, 1859; c) X. Zhou, C. Li, R. Bhandary, Z. Katcharava, F. Du, R. Androsch, A. Marinow, W. H. Binder, *ACS Appl. Eng. Mater.* **2023**, *1*, 1997. d) N. Boaretto, L. Meabe, M. Martinez-Ibañez, M. Armand, H. Zhang, *J. Electrochem. Soc.* **2020**, *167*, 070524; e) X. Yang, J. Liu, N. Pei, Z. Chen, R. Li, L. Fu, P. Zhang, J. Zhao, *Nano-Micro Lett.* **2023**, *15*, 74; f) C. Lu, X. Chen, *Chem. Commun.* **2019**, *55*, 8470.
[18] Y. Preibisch, F. Horsthemke, M. Winter, S. Nowak, A. S. Best, *Chem. Mater.* **2020**, *32*, 2389.
[19] L. Herbers, V. Küpers, M. Winter, P. Bieker, *RSC Adv.* **2023**, *13*, 17947.
[20] L. Chen, J. Fu, Q. Lu, L. Shi, M. Li, L. Dong, Y. Xu, R. Jia, *Chem. Eng. J.* **2019**, *378*, 122245.
[21] S. Qin, Y. Cao, J. Zhang, Y. Ren, C. Sun, S. Zhang, L. Zhang, W. Hu, M. Yu, H. Yang, *Carbon Energy* **2023**, *5*, e316.
[22] C. Li, R. Bhandary, A. Marinow, S. Bachmann, A. C. Poppler, W. H. Binder, *Macromol. Rapid Commun.* **2024**, *45*, 2300464.
[23] A. Heist, S. Hafner, S. H. Lee, *J. Electrochem. Soc.* **2019**, *166*, A873.
[24] A. Campanella, D. Döhler, W. H. Binder, *Macromol. Rapid Commun.* **2018**, *39*, 1700739.
[25] Y. H. Jo, B. Zhou, K. Jiang, S. Li, C. Zuo, H. Gan, D. He, X. Zhou, Z. Xue, *Polym. Chem.* **2019**, *10*, 6561.
[26] M. Alvarez-Tirado, L. Castro, A. Guéguen, D. Mecerreyes, *Batteries Supercaps* **2022**, *5*, 202200049.
[27] Y. Choo, D. M. Halat, I. Villaluenga, K. Timachova, N. P. Balsara, *Prog. Polym. Sci.* **2020**, *103*, 101220.
[28] a) Z. Li, J. Fu, X. Zhou, S. Gui, L. Wei, H. Yang, H. Li, X. Guo, *Adv. Sci.* **2023**, *10*, 2201718; b) X. Zhao, C. Wang, H. Liu, Y. Liang, L. Z. Fan, *Batteries Supercaps* **2023**, *6*, 202200502; c) Z. Song, F. Chen, M. Martinez-Ibanez, W. Feng, M. Forsyth, Z. Zhou, M. Armand, H. Zhang, *Nat. Commun.* **2023**, *14*, 4884.
[29] a) M. L. Lehmann, G. Yang, J. Nanda, T. Saito, *J. Electrochem. Soc.* **2020**, *167*, 070539; b) A. A. Teran, M. H. Tang, S. A. Mullin, N. P. Balsara, *Solid State Ion.* **2011**, *203*, 18.
[30] L. Tang, B. Chen, Z. Zhang, C. Ma, J. Chen, Y. Huang, F. Zhang, Q. Dong, G. Xue, D. Chen, C. Hu, S. Li, Z. Liu, Y. Shen, Q. Chen, L. Chen, *Nat. Commun.* **2023**, *14*, 2301.
[31] a) G. A. Elia, U. Ulissi, S. Jeong, S. Passerini, J. Hassoun, *Energy Environ. Sci.* **2016**, *9*, 3210; b) P. Nürnberg, J. Atik, O. Borodin, M. Winter, E. Paillard, M. Schönhoff, *J. Am. Chem. Soc.* **2022**, *144*, 4657; c) J. Atik, D. Diddens, J. H. Thienenkamp, G. Brunklaus, M. Winter, E. Paillard, *Angew. Chem., Int. Ed.* **2021**, *60*, 11919.
[32] X. Cheng, Y. Jiang, C. Lu, J. Li, J. Qu, B. Wang, H. Peng, *Batteries Supercaps* **2023**, *6*, 202300057.
[33] a) S. Davino, D. Callegari, D. Pasini, M. Thomas, I. Nicotera, S. Bonizzoni, P. Mustarelli, E. Quartarone, *ACS Appl. Mater. Interfaces* **2022**, *14*, 51941; b) Y. Ren, J. Guo, Z. Liu, Z. Sun, Y. Wu, L. Liu, F. Yan, *Sci. Adv.* **2019**, *5*, eaax0648.
[34] N. Sánchez-Ramírez, B. D. Assresahegn, D. Bélanger, R. M. Torresi, *J. Chem. Eng. Data* **2017**, *62*, 3437.
[35] a) L. Long, S. Wang, M. Xiao, Y. Meng, *J. Mater. Chem. A* **2016**, *4*, 10038; b) D. Zhou, D. Shanmukaraj, A. Tkacheva, M. Armand, G. Wang, *Chem* **2019**, *5*, 2326.
[36] a) M. Armand, F. Endres, D. R. MacFarlane, H. Ohno, B. Scrosati, *Nat. Mater.* **2009**, *8*, 621; b) H. Niu, L. Wang, P. Guan, N. Zhang, C. Yan, M. Ding, X. Guo, T. Huang, X. Hu, *J. Energy Storage* **2021**, *40*, 102659.
[37] a) X. Feng, M. Ouyang, X. Liu, L. Lu, Y. Xia, X. He, *Energy Storage Mater.* **2018**, *10*, 246; b) K. Liu, Y. Liu, D. Lin, A. Pei, Y. Cui, *Sci. Adv.* **2018**, *4*, eaas9820.
[38] a) E. Fan, L. Li, Z. Wang, J. Lin, Y. Huang, Y. Yao, R. Chen, F. Wu, *Chem. Rev.* **2020**, *120*, 7020; b) X. Wu, J. Ma, J. Wang, X. Zhang, G. Zhou, Z. Liang, *Global Challenges* **2022**, *6*, 2200067.